LES OF TRANSITIONAL FLOWS USING APPROXIMATE DECONVOLUTION

Philipp Schlatter, Steffen Stolz, Leonhard Kleiser
Institute of Fluid Dynamics
Swiss Federal Institute of Technology ETH Zürich
CH-8092 Zürich, Switzerland
schlatter@ifd.mavt.ethz.ch

ABSTRACT

Large-eddy simulations of transitional incompressible channel flow on comparably coarse grids are performed. Two modifications to the standard Approximate Deconvolution Method (ADM) are proposed and compared to highly resolved DNS calculations. The results demonstrate that it is well possible to simulate transitional flows on the basis of the ADM algorithm. During the initial phase of transition, the models remain inactive and do not disturb the flow development as long as it is still well resolved on the coarse LES grid. During the late stages of transition the model contributions provide necessary additional dissipation.

The results of the modified ADM show excellent agreement with DNS in e.g. the skin friction throughout the transitional phase and the fully developed turbulent channel flow. Moreover, due to the dynamic determination of the model coefficient, no additional ad-hoc constants or adjustments are needed.

INTRODUCTION

Flows undergoing transition to turbulence are of great practical importance, e.g. flows in boundary layers on aircraft wings or intermittent flows around turbine blades. The use of Large-Eddy Simulations (LES) to predict transitional and turbulent flows is appealing as they promise to provide accurate results at greatly reduced computational cost in comparison with fully resolved Direct Numerical Simulations (DNS). However, transitional flows are substantially different from turbulent flows in many respects. Not only is there no fully-developed energy cascade, but also slow growth and subtly complex interactions between base flow and various instability modes can affect the physical changeover from the laminar to the turbulent state and must thus be resolved or modeled reliably.

The physics of forced transition to turbulence in canonical geometries is well understood and there are many experiments, stability theories and simulations available (Kleiser and Zang, 1991; Herbert, 1988).

Only recently, large-eddy simulations of transitional flows have become an important field of research. Nevertheless, a number of successful applications of LES to transitional flows are available, most of them based on the Smagorinsky model (Smagorinsky, 1963). In its original form, Smagorinsky's model is too dissipative and usually relaminarizes transitional flows. Therefore, Piomelli and Zang (1991) introduced an intermittency correction to the eddy-viscosity to decrease the dissipation in (nearly-)laminar regions for their channel flow simulation. Voke and Yang (1995) employed a low-Reynolds number correction to simulate bypass transition. Alternatively, Germano *et al.* (1991) and subsequently Lilly (1992) proposed a *dynamic* Smagorinky model. This class of models has been successfully used, e.g. for transition in incompressible boundary layers by Huai *et al.* (1997) applying the localized dynamic version of Piomelli and Liu (1995). Still using an eddy-viscosity assumption, Ducros *et al.* (1996) introduced the filtered structure function model and applied it successfully to weakly compressible boundary layer flow. In its original form, the structure function model (Métais and Lesieur, 1992) was found too dissipative for transitional flows.

A SGS model suitable to simulate transition should leave the laminar base flow unaffected and only be effective, in an appropriate way, when nonlinear interactions between the resolved modes and the non-resolved scales become important. The initial slow growth phase of the instability waves is mostly sufficiently resolved even on a coarse LES grid.

The aim of the present work is to examine the applicability of the ADM approach to transitional flows. Large-eddy simulations using the approximate deconvolution model (ADM) in the fully-turbulent regime have shown very good agreement with DNS calculations, e.g. for incompressible channel flow (Stolz *et al.*, 2001a), shock/turbulent-boundary-layer interaction (Stolz *et al.*, 2001b). A transitional rectangular jet has been simulated by Rembold *et al.* (2002). As a first step, the present study investigates the simulation of temporal K-type (fundamental) transition in incompressible channel flow, for which extended DNS results are available (Gilbert and Kleiser, 1990). In order to test the performance of the SGS model, the grid resolution for the LES calculations is chosen quite coarse. With such resolution, a computation without model is underresolved in all three spatial directions and the SGS terms are indeed needed.

LES MODELLING

In the ADM approach, the filtered Navier-Stokes equations with deconvolved quantities are used with the unclosed terms and a relaxation term is added to the right-hand side (Stolz *et al.*, 2001a). Equation

$$\frac{\partial \overline{u}_i}{\partial t} + \frac{\overline{\partial u_j^* u_i^*}}{\partial x_j} + \frac{\partial \overline{p}}{\partial x_i} - \frac{1}{Re}\frac{\partial^2 \overline{u}_i}{\partial x_j \partial x_j} = -\chi(I - Q_N * G) * \overline{u}_i \quad (1)$$

is solved together with the filtered incompressibility constraint

$$\frac{\partial \overline{u}_i}{\partial x_i} = 0 \quad (2)$$

Here, an overbar denotes filtered quantities $\overline{u}_i = G * u_i$, a star stands for the approximately deconvolved quantities $u_i^* := Q_N * \overline{u}_i$, G is the discrete primary low-pass filter (defined below) and Q_N its approximate inverse $Q_N = \sum_{\nu=0}^{N}(I - G)^\nu \approx G^{-1}$. The definition of G is based on Stolz *et al.* (2001a) and can be written for equidistant grids in Fourier space (see figure 1) as

$$G(\omega) = 0.625 + 0.5\cos\omega - 0.125\cos 2\omega \quad (3)$$

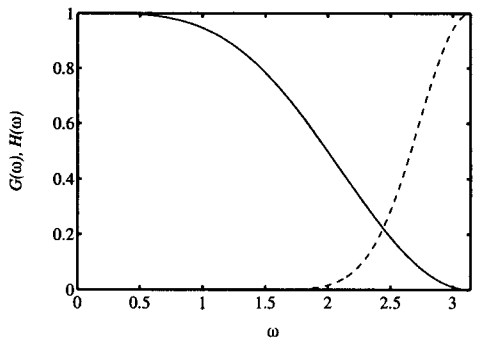

Figure 1: Transfer functions for the different filter (periodic, equidistant grid directions only), $N = 5$. ——— $G(\omega)$ ----$H(\omega) = 1 - Q_N(\omega)G(\omega)$

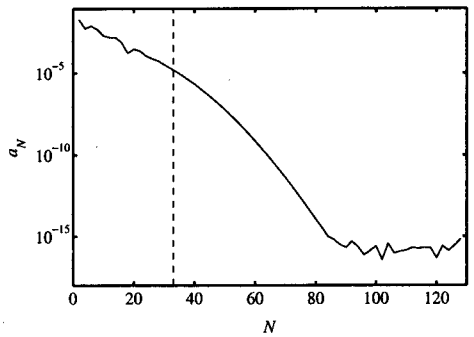

Figure 2: Chebyshev spectrum a_N of the streamwise velocity component of the initial disturbance. The vertical dashed line indicates a wall-normal resolution of $N = 33$.

The definition is extended to non-equidistant grids in the wall-normal direction by assuring that all moments up to second order are vanishing. For this reason the parabolic laminar base flow profile is invariant with respect to the filter operation. Moreover, the high-pass filter $H = I - Q_N * G$ is at least of order $\mathcal{O}(\Delta^{r(N+1)})$ with Δ being the grid size, N the deconvolution order and r the order of the primary filter. The latter is at least 3 for the primary filter G used herein.

NUMERICAL IMPLEMENTATION AND PARAMETER SETTINGS

The simulations use a parallel implementation of a Fourier-Chebyshev spectral method with periodic boundary conditions in the streamwise and spanwise directions together with no-slip conditions at the walls. A constant flow rate is maintained, and the nonlinear terms are computed with full dealiasing in all spatial directions. The divergence-free condition is enforced exactly by an influence-matrix technique (Kleiser and Schumann, 1984). Time advancement is done by a semi-implicit Runge-Kutta/Crank-Nicolson scheme. The initial disturbances for the transition simulations consist of a two-dimensional (stable) Tollmien-Schlichting (TS) wave with intensity 3% and two superimposed oblique (stable) three-dimensional waves with intensity 0.1% as in the fully resolved DNS by Gilbert and Kleiser (1990). The Reynolds number based on the bulk velocity and the channel half-width is $Re = 3333$. For the statistically stationary results of fully-developed turbulent channel flow, the data is averaged from time $t = 250$ to $t = 500$ well after the transitional phase. Because the Reynolds number of the results for the turbulent channel flow with $Re_\tau \approx 210$ ($Re = 3333$) is similar to $Re_\tau \approx 180$ ($Re = 2800$) (Moser *et al.*, 1999), we present results for $Re_\tau \approx 210$ only.

In figure 2 a Chebyshev spectrum of the streamwise velocity component of the initial disturbance is shown. As it can be inferred from the figure, the disturbances are fully resolved (with about 15 decimals machine precision) for $N \approx 90$. For $N > 25$ the energy content of the modes is monotonically decreasing, indicating that the minimum resolution to resolve the initial disturbance lies just above $N = 25$. For this reason a minimum wall-normal resolution of $N = 33$ should chosen for an LES. To further validate this point, two simulations with full resolution ($128^2 \times 129$ grid points) were conducted starting from fields with resolution $32^2 \times 33$ at $t = 0$ and $t = 80$, respectively. Both showed no significant difference in the integral quantities like skin friction and shape factor during transition compared to the

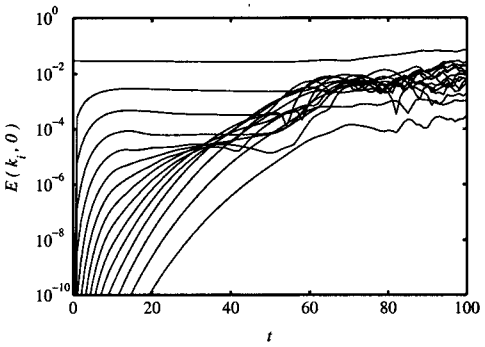

Figure 3: Evolution of 2D Fourier modes $(k_i, 0)$ during the initial states of transition. SGS model is standard ADM with deconvolution, but without relaxation ($\chi = 0$).

reference DNS calculation ($128^2 \times 129$ grid points for simulation and initial condition). Moreover, it can be concluded that the initial phase of the saturated Tollmien-Schlichting wave is sufficiently resolved with only 33 wall-normal points. Further test calculations were conducted to confirm the accuracy of the results with respect to the choice of the time step.

RESULTS

Standard ADM

For both laminar and turbulent flow, the standard ADM gives good results. However, initial tests using ADM in its original form (Stolz *et al.*, 2001a) have confirmed the expectation that it cannot directly be applied to simulate transitional flows on very coarse grids in which the initial state consists of a laminar base flow with superimposed small-amplitude disturbances. The problem is mainly due to improper interaction of deconvolution for the nonlinear terms and the relaxation term. Figure 3 shows the evolution of the 2D Fourier modes with vanishing relaxation term $\chi = 0$. The physical solution at this stage of development ($t < 100$) consists of a saturated 2D wave, which exhibit a geometric progression to higher wavenumbers, with each of the Fourier modes slowly decaying in time (Gilbert and Kleiser, 1990), see also figure 8. However, the influence of the deconvolution on the laminar solution is such that small-scale perturbations are amplified until these are dominating the flow field. The reason for this is the repeated application of the filter G in regions close to the wall. Fulfilling the wall

boundary conditions can lead to oscillations in the near-wall region. Note that this phenomenon only occurs if three-dimensional filtering is used and the wall-normal resolution is fairly coarse. For example, using 48 or more points in the wall-normal direction, the deconvolution gives good results even close to the wall due to the lower energy content of the modes near the cutoff (see figure 2). Applying the filter operation in Chebyshev spectral space instead of a real-space implementation does not remedy these deficiencies. Therefore, it seems to be inherent to such coarse grids. It should be noted again that the grid was deliberately chosen very coarse.

Modified ADM

To overcome the above-mentioned deficiencies of the standard ADM procedure, two alternative variants have been developed. Both of these were found to be suitable for LES of transitional flow.

LES(a) Instead of using three-dimensional filtering and deconvolution, only two-dimensional filtering in the homogeneous wall-parallel directions is applied. The two-dimensional deconvolution operator is maintained all the way through the transitional and turbulent phases. Herewith, the advantages of the ADM technique are retained, although this model is not as general as the original formulation since it is restricted to filtering in two dimensions only.

LES(b) The three-dimensional filter definition is retained to evaluate the relaxation term, but the non-linear terms are evaluated as $\frac{\partial \overline{u}_j \overline{u}_i}{\partial x_j}$, as in a coarse-grid DNS. Note that with this procedure the quantity $\overline{u}_i$ has to be considered as filtered by spectral cut-off to grid resolution. This modification is still as general as the standard ADM procedure but does not use deconvolved quantities for the non-linear terms.

For both options, the dynamic determination of the relaxation parameter χ follows the standard formulation (Stolz *et al.*, 2001b)

$$\chi(t+\Delta t) = \chi(t) \frac{F_2(t+\Delta t)|_{\chi=0} - F_2(t)}{F_2(t+\Delta t)|_{\chi=0} - F_2(t+\Delta t)|_{\chi=\chi(t)}} \quad (4)$$

where $F_2(t) = F_2(H*\overline{u}_i, t)$ is the second-order velocity structure function, computed from the high-pass filtered velocity field $H*\overline{u}_i$. This dynamic determination of χ aims at keeping the energy at small scales constant, for which $F_2(H*\overline{u}_i)$ is a measure. Usually, χ is updated only every couple of time steps, but changing this interval somewhat has negligible influence. In order to ascertain numerical stability, χ needs to be clipped to $0 \leq \chi \leq 1/\Delta t$. Moreover, a filter operation was applied to smoothen χ in regions where it strongly varies in space.

Results are shown for the simulations given in table 1. All computations were started at $t = 0$ with the initial condition described in section 2 and integrated up to at least a non-dimensional time $t = 500$. For LES(a) and LES(b) the term $-\chi \cdot (I - Q_N * G) * \overline{u}_i$ was computed in real space with full dealiasing. LES(c) denotes the dynamic Smagorinsky model (Lilly, 1992), included here for reference.

Transitional phase. During the initial phase ($t < 100$) the saturated two-dimensional Tollmien-Schlichting wave is dominating, thus all integral quantities like Re_τ remain on their laminar values. In the secondary instability phase (Herbert, 1988), coinciding with the visible onset of transition ($t \approx 100$), the typical Λ-shaped vortices are generated and elongated ($t \approx 120$). This leads to the distinct peak-valley splitting (Gilbert and Kleiser, 1990). In the following "spike stage" the flow is dominated by strong wall-normal shear layers which rapidly break down to turbulence, first in the peak plane and shortly thereafter in the valley regions. Although the Λ-vortices can be identified in all the different simulations, the time t of the breakdown is quite different for the various computations. This is shown by figure 4 which depicts the temporal evolution of the Reynolds number Re_τ based on the friction velocity and the channel half-width, averaged over the two walls. The onset of transition and the initial growth of Re_τ is still comparable for all simulations, they begin to separate during the spike stage ($t = 140$). Furthermore, the skin friction peak value is similar and the well-known overshoot of Re_τ of about 15% is visible for both DNS and LES(a) and LES(b). The formation of fully developed turbulence seems to proceed on the same time scale. The stationary values of Re_τ after transition ($Re = 3333$) are given in table 1.

Table 1: Temporally and spatially averaged skin friction Re_τ obtained for the different simulations of fully developed turbulent channel flow.

Re_τ for $Re =$	2800	3333	
LES(a) $32^2 \times 33$, 2D filt./deconv.	180.4	214.2	—·—
LES(b) $32^2 \times 33$, only 3D relax.	179.7	209.8	- - - -
LES(c) $32^2 \times 33$, dyn. Smag.	170.7	201.8	·····
coarse grid DNS $32^2 \times 33$	201.9	220.6	—o—
fully-resolved DNS $128^2 \times 129$	177.8	212.5	———

The shape factor H_{12} is a quantity that gives an idea of the reorganization of the mean velocity profile averaged over wall-parallel planes (figure 5). Starting from the value $H_{12} = 2.5$ of the laminar base flow profile all simulations reach the turbulent value at around the same time $t = 170$.

The mean-velocity deficit in the middle of the channel, seen from Re_{CL} in figure 6, shows again at least two distinct paths from the laminar to the turbulent values.

It is common to all these results that the coarse-grid DNS and the 2D filtered LES(a) are always going through transition at earlier times than the fully-resolved DNS and LES(b). LES(c) seems to first follow the route of the coarse-grid DNS and then to change to the path of the fine-grid DNS.

Better insight can be gained by looking at the velocity fluctuations $u_{rms,max}$, the wall-normal maximum of the streamwise average of u_{rms}, given for the valley plane in figure 7. It is obvious that the coarse-grid DNS and LES(a) are close together, indicating that the SGS model is still inactive until $t \approx 150$. For LES(b) already at $t \approx 120$ some minor differences can be observed and due to dissipative SGS influence the u_{rms} peak at $t = 160$ is accurately predicted. The Smagorinksy model again follows a route in between the two DNS calculations. In the peak plane (not shown here), the phase of intense fluctuation is observed at the same time for all simulations ($t \approx 150$).

Detailed analysis of LES(b). LES(b) follows the fully-

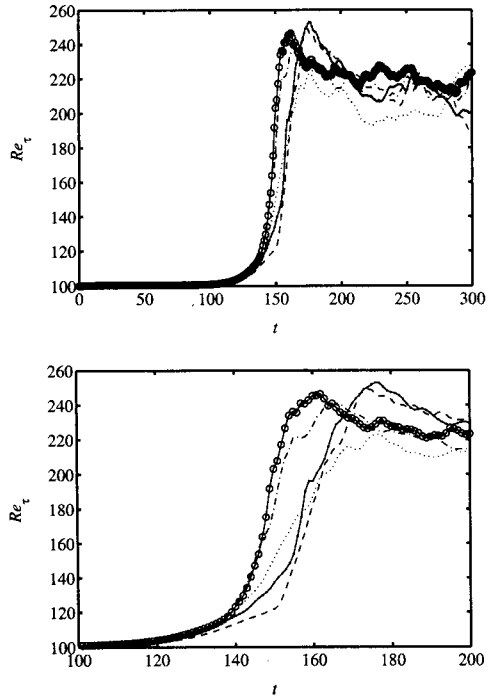

Figure 4: Evolution of Re_τ averaged in a wall-parallel plane during the transitional phase ($Re = 3333$). Line caption see table 1.

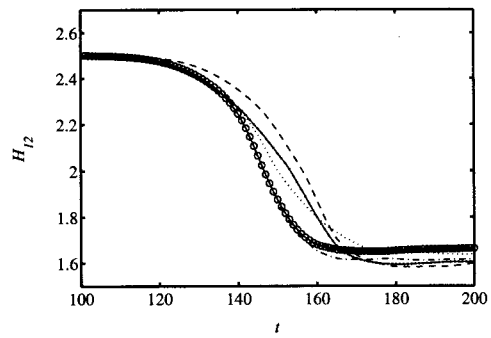

Figure 5: Evolution of the shape factor H_{12} averaged in a wall-parallel plane during the transitional phase ($Re = 3333$). Line caption see table 1.

resolved DNS best and shows significant improvement of the results over the coarse-grid DNS and the other models LES(a) and LES(c). It is therefore interesting to look at the evolution of the Fourier components that correspond to the 2D waves of the saturated Tollmien-Schlichting wave. Figure 8 shows both the DNS and the LES(b) calculation. The modes that are on an energy level above 10^{-5} are even for the LES on the respective DNS level. However, higher modes contain more energy than in the DNS and are very noisy. This is interesting from that respect that these oscillations must clearly be attributed to the SGS model. On the other hand, these perturbations do not grow in time and do not lead to inaccurate integral results. These disturbances originate close to the wall boundaries where the three-dimensional high-pass filter used for the relaxation term is difficult to apply.

The evolution of the dynamic coefficient for the relaxation term χ is shown in figures 9 and 10. Every five full

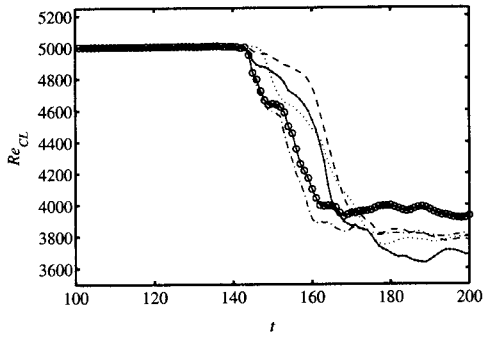

Figure 6: Evolution of Re_{CL} averaged in a wall-parallel plane during the transitional phase ($Re = 3333$). Line caption see table 1.

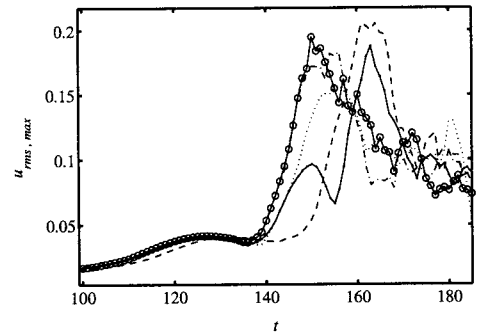

Figure 7: Evolution of $u_{rms,max}$ during the transitional phase ($Re = 3333$). The wall-normal maximum of the streamwise average of u_{rms} is shown. Line caption see table 1.

Runge-Kutta time steps, χ is updated according to equation (4). This definition was derived for fully-turbulent flows for which it aims at keeping in equilibrium the energy content of the small scales. The consequence can be seen in figure 9 for $t < 150$: Since the energy of the small scales is growing at these times due to physical interactions, the relaxation term is growing as well to counteract the generation of small-scale energy. However, the total influence of the relaxation term $-\chi H * \overline{u}_i$ is still very limited due to the fact that $H * \overline{u}_i$ is small. Only when the energy cascade has extended to the smallest resolved scales the equilibrium between production and dissipation becomes relevant, indicated by the statistically constant values of χ ($t > 160$). In figure 10, wall-normal profiles of χ are shown. During the phase when the saturated TS-wave is dominating the flow a maximum is visible close to the wall ($t = 60$), whereas during the secondary instability phase ($t = 130$) the maxima have moved further away from to wall. In the fully-developed turbulent channel, χ is fairly constant across the channel with slight decrease close to the wall. This is actually desired as the influence of the model close to the wall should be smaller.

Fully turbulent phase. In table 1, the averaged values for Re_τ are also given for $Re = 2800$ (see Moser *et al.* (1999)). For the $Re = 3333$ cases, statistical averaging is performed for $t = 250 - 500$. The mean turbulent velocity profiles are depicted in figure 11 and the velocity fluctuations are shown in figure 12.

It is obvious that the coarse-grid DNS overpredicts the stationary value of Re_τ by approximately 10% compared

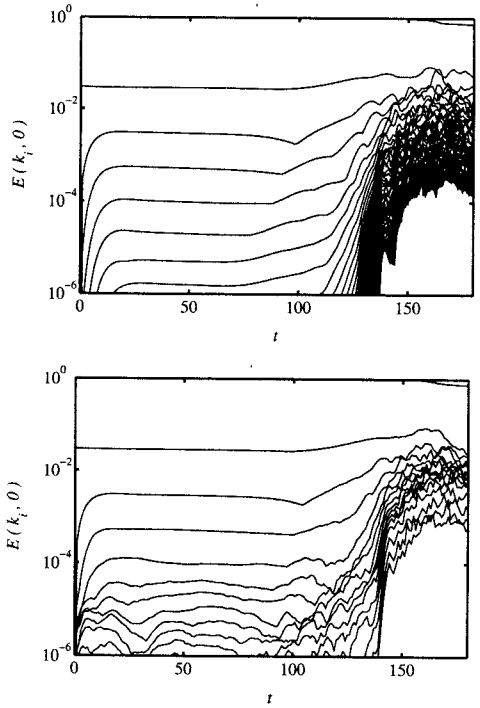

Figure 8: Evolution of the Fourier modes corresponding to two-dimensional waves during the transitional phase (Re = 3333, LES(b)). *top* fully-resolved DNS $128^2 \times 129$, *below* LES(b) $32^2 \times 33$

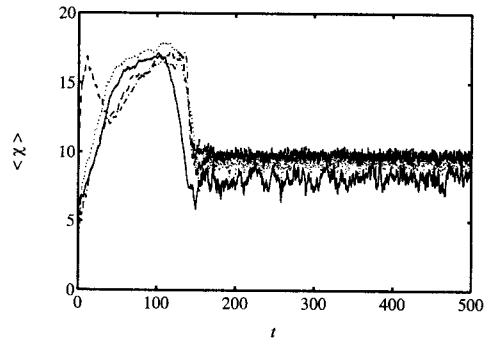

Figure 9: Evolution of χ averaged wall-parallel planes during the transitional phase (Re = 3333, LES(b)). ——— $z = -1$, - - - - $z = 0$, ····· $z = 0.9$ —·— $z = 0.65$

to the resolved DNS. This is explained by the fact that the numerical scheme used for the computations provides no inherent numerical dissipation. Both model calculations LES(a) and LES(b) provide a much better prediction of the wall friction. The dynamic Smagorinsky model LES(c) does similarly, although it seems to be slightly too dissipative. A similar conclusion can be drawn from the mean velocity profile; especially LES(b) agrees very well with the fully-resolved DNS and the theoretical values.

The prediction of the velocity fluctuations (figure 12) for the dynamic Smagorinsky model LES(c) are not very accurate, whereas the use of the ADM cases LES(a) and LES(b) shows a substantial improvement. Again, LES(b) (no deconvolution) is very close to the values of the fine-grid DNS calculation. LES(a) is less accurate leading to the conclusion that the capturing of three-dimensional effects in relaxation and deconvolution are important (compare also to

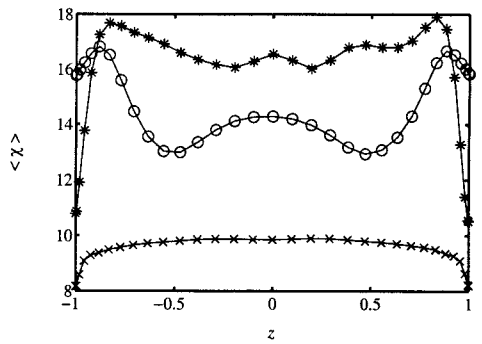

Figure 10: Evolution of χ averaged in wall-parallel planes during the transitional phase (Re = 3333, LES(b)). $\circ$ $t = 60$, $*$ $t = 130$, $\times$ averaged $t = 250 - 500$

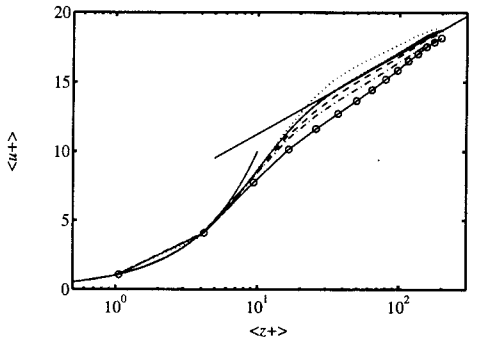

Figure 11: Averaged velocity profile $< u^+ >$ scaled with wall units in the fully turbulent case (Re = 3333). Line caption see table 1.

three-dimensional filtering and deconvolution in Stolz *et al.* (2001a)).

CONCLUSIONS

Several large-eddy simulations of transitional incompressible channel flow have been performed. In order to be able to work on the very coarse grid deliberately chosen, the standard ADM methodology had to be adapted due to properties of the deconvolution in the wall-normal direction. Two new variants of the original ADM algorithm are proposed and compared to coarse- and fine-grid DNS calculations as well as results of the dynamic Smagorinksy model.

The results obtained indicate that it is well possible to simulate transitional wall-bounded flows on the basis of the modified ADM method. During the early stages of transition, the results of the coarse-grid DNS calculations, which have sufficient resolution for this stage of flow development, can be recovered. This indicates that the LES model is inactive there. During the rapid mean flow development, the model contributions are beginning to provide additional dissipation. The results demonstrate that a proper treatment of each spatial direction should be used in order to faithfully represent the relevant physical features such as the local gradients. Moreover, the LES model is formulated in a more general way.

The neglect of the deconvolution in the model LES(b) is a step towards a more simple subgrid model which provides dissipation based on a filtering approach. A further investigation aiming at a more versatile procedure for an easier dynamic determination of the relaxation parameter χ

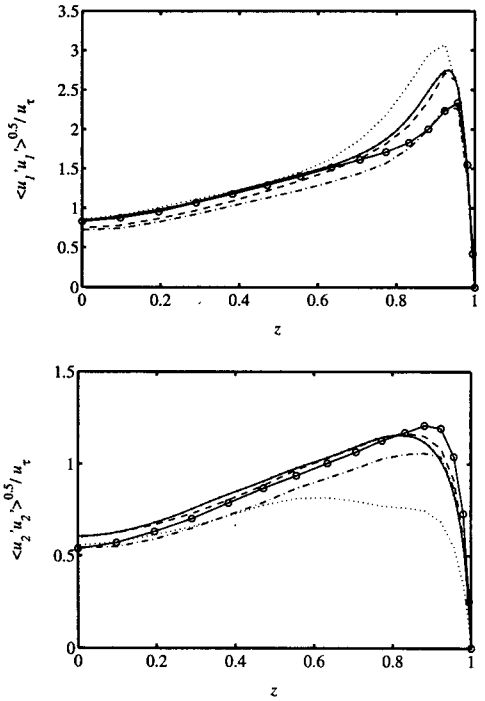

Figure 12: Averaged velocity fluctuations in the fully turbulent case ($Re = 3333$). Line caption see table 1. *top* $< u_1'u_1' >^{0.5} /u_\tau$, *below* $< u_2'u_2' >^{0.5} /u_\tau$.

is currently in progress.

The LES models presented herein are completely dynamic in space and time such that no ad-hoc constants or adjustements are needed. This self-adaptation to the current flow situation is very important for all types of transitional flows. An interesting extension of the present work will be spatial simulations with more complex flow situations like separation.

ACKNOWLEGEMENTS

The authors are indebted to Professor N. A. Adams (TU Dresden) for many helpful discussions during the initial phase of the project. This work was supported by the Swiss National Science Foundation and the Swiss Center for Scientific Computing (CSCS). Calculations have been performed at CSCS.

REFERENCES

Ducros, F., Comte, P., and Lesieur, M., 1996. "Large-eddy simulation of transition to turbulence in a boundary layer developing spatially over a flat plate." *J. Fluid Mech.*, vol. 326, pp. 1–36.

Germano, M., Piomelli, U., Moin, P., and Cabot, W. H., 1991. "A dynamic subgrid-scale eddy viscosity model." *Phys. Fluids*, vol. 3(7), pp. 1760–1765.

Gilbert, N. and Kleiser, L., 1990. "Near-wall phenomena in transition to turbulence." In Kline, S. J. and Afgan, N. H., eds., *Near-Wall Turbulence - 1988 Zoran Zarić Memorial Conference*, pp. 7–27. Hemisphere.

Herbert, T., 1988. "Secondary instability of boundary layers." *Ann. Rev. Fluid Mech.*, vol. 20, pp. 487–526.

Huai, X., Joslin, R. D., and Piomelli, U., 1997. "Large-eddy simulation of transition to turbulence in boundary layers." *Theoret. Comput. Fluid Dynamics*, vol. 9, pp. 149–163.

Kleiser, L. and Schumann, U., 1984. "Spectral simulation of the laminar-turbulent transition process in plane Poiseuille flow." In Voigt, R. G., ed., *Spectral Methods for partial differential equations*, pp. 141–163. SIAM, Philadelphia.

Kleiser, L. and Zang, T. A., 1991. "Numerical simulation of transition in wall-bounded shear flows." *Annu. Rev. Fluid Mech.*, vol. 23, pp. 495–537.

Lilly, D. K., 1992. "A proposed modification of the Germano subgrid-scale closure method." *Phys. Fluids*, vol. A 4(3), pp. 633–635.

Métais, O. and Lesieur, M., 1992. "Spectral large-eddy simulation of isotropic and stably stratified turbulence." *J. Fluid Mech.*, vol. 239, pp. 157–194. 97.

Moser, R. D., Kim, J., and Mansour, N. N., 1999. "Direct numerical simulation of turbulent channel flow up to $Re_\tau = 590$." *Phys. Fluids*, vol. 11(4), pp. 943–945.

Piomelli, U. and Liu, J., 1995. "Large-eddy simulation of rotating channel flows using a localized dynamic model." *Phys. Fluids*, vol. 7(4), pp. 839–848.

Piomelli, U. and Zang, T. A., 1991. "Large-eddy simulation of transitional channel flow." *Comp. Phys. Comm.*, vol. 65, pp. 224–230.

Rembold, B., Adams, N. A., and Kleiser, L., 2002. "Direct numerical simulation of a transitional rectangular jet." *Int. J. Heat Fluid Flow*, vol. 23(5), pp. 547–553.

Smagorinsky, J., 1963. "General circulation experiments with the primitive equations." *Mon. Weath. Rev.*, vol. 91(3), pp. 99–164.

Stolz, S., Adams, N. A., and Kleiser, L., 2001a. "An approximate deconvolution model for large-eddy simulation with application to incompressible wall-bounded flows." *Physics of Fluids*, vol. 13(4), pp. 997–1015.

Stolz, S., Adams, N. A., and Kleiser, L., 2001b. "The approximate deconvolution model for large-eddy simulations of compressible flows and its application to shock-turbulent-boundary-layer interaction." *Phys. Fluids*, vol. 13(10), pp. 2985–3001.

Voke, P. and Yang, Z., 1995. "Numerical study of bypass transition." *Phys. Fluids*, vol. 7(9), pp. 2256–2264.